Estimation of Transmembrane Potentials from Phase Equilibria of Hydrophobic Paramagnetic Ions†

David S. Cafiso and Wayne L. Hubbell*,‡

ABSTRACT: Positively charged hydrophobic spin labels have been synthesized which respond to transmembrane potentials in sonicated liposomes. Electron paramagnetic resonance spectroscopy is used to show that the distribution of these probes between aqueous and membrane phases changes as a function of transmembrane potential. When liposomes are made more inside-negative, the fraction of membrane associated probe increases while the fraction of probe in the aqueous phase decreases. The results are in quantitative agreement with a simple equilibrium thermodynamic theory which allows estimation of absolute transmembrane potentials in phospholipid vesicles.

Biological membranes are intimately involved in a number of energy transducing and regulatory processes. In many cases these processes are associated with steady state or transient transmembrane potentials (potentials resulting from a net charge separation across the membrane). As a result, techniques which measure and characterize these potentials can be particularly useful in the study of membrane phenomena. Unfortunately, microelectrode methods are restricted to use in relatively large systems and potentials across the membranes of liposomes, membrane vesicles, and reconstituted membrane systems are inaccessible with these techniques.

Estimates of transmembrane potentials in these smaller structures have generally been obtained by techniques utilizing fluorescent dyes of the oxonol, cyanine, and merocyanine types (see Waggoner, 1976, for a review), safranine dyes (Akerman and Saris, 1976; Akerman and Wikström, 1976), and radioactive hydrophobic ions (Bakeeva et al., 1970). The mechanisms responsible for the potential-dependent optical changes in the dyes are at best only qualitatively understood (Waggoner, 1976) and in practice their use is based on empirical calibration. Determination of the inside-outside distribution of radioactive hydrophobic ions, although of general applicability, is of relatively low time resolution and limited to the study of equilibrium or steady-state potentials.

The first spin-label determination of transmembrane potential was presented by Kornberg et al. (1972). In this approach, spin-label derivatives of weak acids are used to sense pH gradients which develop as a result of transmembrane potentials in proton permeable systems. In this report, we discuss a new, rapid technique for directly estimating transmembrane potentials in phospholipid vesicles in which EPR[1] spectroscopy is used to monitor the distribution of a hydrophobic nitroxide cation between aqueous and membrane phases. The structures of the paramagnetic probes used for transmembrane potential measurements are shown below.

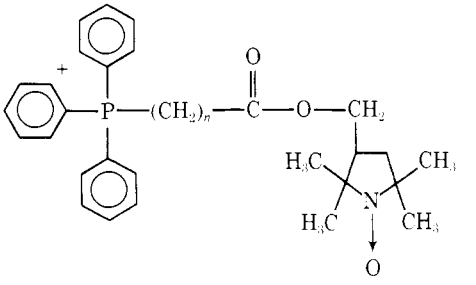

I(n)

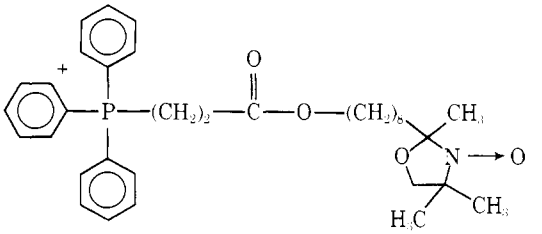

II

It will be shown that the distribution of these phosphonium spin labels between the membrane and aqueous solution is dependent on transmembrane potential, and that the potential dependence is in good agreement with a simple thermodynamic theory.

Experimental Section

Materials. Phosphatidylcholine (PC) was prepared according to the method of Singleton et al. (1965). The final product was stored at −20 °C in chloroform under nitrogen at a concentration of 75 mg/mL. Valinomycin was obtained from Sigma Chemical Co., St. Louis, Mo. *N,N,N*-Trimethyl-*N*-tempoylammonium bromide was a gift of Carole Hamilton. 3-Hydroxymethyl-2,2,5,5-tetramethylpyrrolidine-1-oxyl was prepared according to Gaffney (1976). 2-(8-Carboxyoctyl)-2-methyl-4,4-dimethyl-3-oxazolidinyloxyl was prepared from 10-ketomethylhendecanoate according to the method of Keana et al. (1967). 10-Ketomethylhendecanoate was a gift of James Cason. 3-Carboxypropyltriphenyl-

† From the Department of Chemistry, University of California, Berkeley, California 94720. *Received August 4, 1977.* This investigation was supported by National Institutes of Health Grant EY00729, The Alfred P. Sloan Foundation, the Camille and Henry Dreyfus Foundation, and the du Pont Science Grant to Chemistry.

‡ Alfred P. Sloan Foundation Fellow and Dreyfus Foundation Scholar.

[1] Abbreviations used are: EPR, electron paramagnetic resonance; PC, phosphatidylcholine; DCC, dicyclohexylcarbodiimide; TLC, thin-layer chromatography; ANS, 8-anilino-1-naphthalenesulfonic acid; CCCP, carbonyl cyanide *m*-chlorophenylhydrazone; tempoyl radical ≡

0006-2960/78/0417-0187$01.00/0

phosphonium chloride and 4-carboxybutyltriphenylphosphonium bromide were prepared according to Denney and Smith (1962).

Synthesis of I(n). The desired carboxyalkyltriphenylphosphonium salt (0.002 mol) was added to 3-hydroxymethyl-2,2,5,5-tetramethylpyrrolidine-1-oxyl (0.002 mol) in a minimum amount of dry dimethylformamide (approximately 5 mL). The reactants were coupled by the addition of 0.002 mol of DCC with stirring at 0 °C. After the addition of DCC, the reaction was allowed to warm to room temperature and stand for 16 h. The reaction mixture was filtered to remove precipitated dicyclohexylurea and the filtrate diluted into 40 mL of ether. The ether-insoluble product was collected by centrifugation, dissolved in a minimum volume of $CHCl_3$, and loaded on a column (22 × 150 mm) of silica gel packed in chloroform. The column was eluted with chloroform containing increasing amounts of methanol. A major yellow band which eluted with 5% methanol in chloroform was collected and the solvent removed by rotary evaporation. The paramagnetic product gave a single spot silica gel TLC when developed with chloroform:methanol 3:1 (R_f approximately 0.6). The two paramagnetic esters synthesized in this fashion, spin labels I(2) and I(3), were very hygroscopic yellow solids and were obtained in approximately 30% yield based on the carboxyalkyltriphenylphosphonium salt. Infrared spectra of these compounds had the characteristic ester carbonyl absorption at 1735 cm^{-1} in addition to the phenylphosphonium absorptions at 1000, 1110, and 1430 cm^{-1}.

Synthesis of II. 2-(8-Carboxyoctyl)-2-methyl-4,4-dimethyl-3-oxazolidinyloxyl (1.0 g; 0.0033 mol) was dissolved in approximately 20 mL of dry ether and lithium aluminum hydride (95 mg; 0.005 mol) was added in small portions with rapid stirring over a period of 30 min. After complete addition of the lithium aluminum hydride, the mixture was stirred for 30 min, 20 mL of saturated sodium sulfate was added, the separated ether phase was collected and dried over anhydrous sodium sulfate, and the solvent removed under vacuum. The resulting yellow oil was chromatographed on silica gel, eluting with 1% (v/v) methanol in chloroform. The single yellow band was collected and the solvent removed to yield 0.4 g of a yellow oil. Thin-layer chromatography (silica gel) of the product showed a single paramagnetic spot when developed with either chloroform (R_f 0.6) or acetone:hexane 1:9 (v/v) (R_f 0.1). The product gave a positive test for primary alcohol on TLC when detected with vanillin reagent (Stahl, 1969). The infrared spectrum of the compound was consistent with the expected primary alcohol 2-(8-hydroxyoctyl)-2-methyl-4,4-dimethyl-3-oxazolidinyloxyl and had a strong absorption at 3400 cm^{-1}. This compound (0.22 g; 0.0008 mol) and 3-carboxypropyltriphenylphosphonium chloride (0.3 g; 0.0008 mol) were dissolved together in approximately 2 mL of dry dimethylformamide. The solution was transferred into a vial containing DCC (0.167 g; 0.0008 mol) and mixed until solution was complete. After standing 12 h at room temperature, the precipitated dicyclohexylurea was removed by centrifugation and 20 mL of ether was added to precipitate the phosphonium salt. The resulting viscous, yellow oil was purified by chromatography on silica gel, eluting with 6% methanol in acetone (v/v). The single yellow band was collected and the solvent removed under vacuum to yield a hydroscopic yellow solid. TLC on silica gel showed a single paramagnetic spot when developed with either acetone (R_f 0.2) or chloroform:methanol 3:1 (v/v) (R_f 0.6). The infrared spectrum showed the expected ester carbonyl adsorption at 1735 cm^{-1} and bands at 1000, 1110, and 1430 cm^{-1} characteristic of quaternary alkyltriphenylphosphonium salts.

Preparation of Phospholipid Vesicles. Aliquots of PC were removed from the stock lipid solution in chloroform and the solvent was removed under a flow of nitrogen. The lipid was further dried in a vacuum desiccator. The dry PC was suspended in the appropriate salt solution (see below) and sonicated (Sonifier, Heat Systems-Ultrasonics, Inc., Plainview, N.Y.) for approximately 20 min at a power of 35 W in an ice bath under nitrogen flow until the lipid suspension became nearly clear (times varied with sample size). The sonicated lipid was then centrifuged for 30 min at 31 000g to remove the titanium dust from the sonicator tip and small amounts of unsonicated lipid. The preparation of negatively stained vesicles for electron microscopy was as previously described (Castle and Hubbell, 1976).

Vesicles prepared for binding measurements were sonicated in a solution containing 225 mM Na^+, 225 mM K^+, 225 mM SO_4^{2-} plus 50 mM sodium phosphate buffer, pH 6.8. For these measurements, the sonicate contained a high concentration of lipid (15% w/v) and was diluted with the above salt solution to achieve the desired final vesicle concentrations. A quantitative determination of the phosphatidylcholine concentration after sonication and centrifugation was obtained by extraction of the PC and subsequent phosphate analysis. The lipid extraction was carried out on a 0.1-mL aliquot of a 1000-fold diluted sample of the concentrated sonicate according to Folch et al. (1957). The organic phase was evaporated under a flow of nitrogen and phosphate analysis (Chen et al., 1956) was carried out on the residues ashed 60 min in refluxing 70% perchloric acid.

For transmembrane potential measurements, vesicles were prepared by sonication of PC (5% w/v) in either *high potassium* (450 mM K^+, 225 mM SO_2^{2-}, plus 50 mM sodium phosphate, pH 6.8) or *high sodium* (440 mM Na^+, 10 mM K^+, 225 mM SO_4^{2-}, plus 50 mM sodium phosphate, pH 6.8).

Generation of Transmembrane Potentials. Vesicles having transmembrane K^+ gradients with ratios $(K^+)_{in}/(K^+)_{out}$ of 1/1, 3/1, 10/1, 45/1, and 90/1 were obtained by passing vesicles prepared by sonication in *high potassium* through a column (180 × 8 mm) of Bio-Gel A-0.5m which was equilibrated with a buffer containing the desired concentration of $(K^+)_{out}$, the ionic strength and osmolarity being adjusted to equal that of the internal vesicle solution by addition of Na_2SO_4. For example, to obtain a ratio of $(K^+)_{in}/(K^+)_{out}$ = 10/1, vesicles containing 450 mM K^+, 225 mM SO_4^{2-}, plus 50 mM sodium phosphate were passed through a column which was equilibrated with 45 mM K^+, 405 mM Na^+, 225 mM SO_4^{2-} plus 50 mM sodium phosphate, pH 6.8. The efficiency of salt exchange on the column was evaluated by assaying K^+ in the effluent. Column fractions were tested for K^+ by the presence of turbidity that developed upon the addition of tetraphenylborate. In the presence of high Na^+, this method was sufficiently sensitive to detect K^+ concentrations of 0.5 mM. For vesicles sonicated in 450 mM K^+ and passed through a column containing 450 mM Na^+, there was approximately 2 mL separating the trailing edge of the vesicle peak (detected by light scattering) and the free K^+ peak. The leading vesicle peak eluted with the void volume (about 2.5 mL). In all cases, only the leading fraction of the vesicle peak was selected. Vesicles having transmembrane K^+ gradients with ratios $(K^+)_{in}/(K^+)_{out}$ of 1/45, 1/15, 1/4.5, and 1/1 were obtained in an analogous manner from vesicles prepared in *high sodium*. Transmembrane potentials were developed in all cases by the addition of valinomycin to vesicles with transmembrane K^+ gradients. In this manner vesicles for which $(K^+)_{in}/(K^+)_{out}$ > 1 gave rise to inside negative potentials and vesicles for which

$(K^+)_{in}/(K^+)_{out} < 1$ gave rise to inside positive potentials. Valinomycin was added to the vesicle preparations from a stock solution (1 mM valinomycin in ethanol) to a final concentration of 10^{-6} M and the vesicles were allowed to stand at room temperature for about 90 min. Ethanol without valinomycin was also added to similar vesicle preparations to obtain a "control" group. The spin-labeled probe was then added from a stock solution at 2×10^{-3} M in the same exterior buffer as the vesicle preparation to a final concentration of 2×10^{-5} M. The expected equilibrium potentials were calculated from the known ratios of $(K^+)_{in}/(K^+)_{out}$ according to the Nernst equation after correcting for the effects of proton permeation and K^+ movement as described by Kornberg et al. (1972).

EPR Measurements and Analysis of Spectra. EPR measurements of vesicle preparations were made with a Varian E-line Century Series X-band EPR spectrometer; samples of approximately 100 μL were placed in a quartz flat cell, and microwave power to the cavity was set at 5 mW; modulation was 0.5 G peak to peak. For measurements at 0 °C, a stream of temperature regulated nitrogen gas was passed over the samples contained in a quartz Dewar fitted inside the EPR cavity.

As will be discussed below, the spectra of spin-labels I(n) and II in suspensions of phospholipid vesicles are superpositions of broad and narrow spectral components arising from labels bound to vesicles and free in aqueous solution, respectively. The information that will be required from the composite spectra is the ratio of bound-to-free spin populations. The extraction of this data from the spectra was performed according to Castle and Hubbell (1976). Briefly, the peak-to-peak amplitude of the high-field resonance line ($I = -1$) of 2×10^{-5} M $I(n)$ in aqueous solution is calibrated in terms of nanomoles of spin. In samples containing vesicles and the same total amount of spin, the amplitude of the high-field resonance of the sharp component directly measures the amount of free spin. Since the total amount of spin is known, the contributions from the bound signal and the ratio of the bound-to-free label are readily calculated. Amplitudes of the high-field resonance were reproducible to within 5% after removal and replacement of identical samples in the microwave cavity.

Measurement of Internal Vesicle Volume. The internal vesicle volume was estimated in a manner similar to that described by Kornberg and McConnell (1971). Egg PC was sonicated in a solution containing 150 mM K^+, 300 mM Na^+, 225 mM SO_4^{2-}, 50 mM sodium phosphate buffer (pH 6.8), and [^{3}H]sucrose. The final concentration of egg PC was 5% w/v. Approximately 0.25 mL of the sonicate was loaded onto a column of Sephadex G-25 (250 × 8 mm) and eluted with the same salt solution without sucrose. The vesicles with trapped sucrose eluted at the void volume followed by a peak of free sucrose. The ratio of vesicle internal volume to external volume in the sonicate was taken as the ratio of the radioactivity in the vesicle peak to that of the free sucrose peak.

Ascorbate Reduction Experiments. Spin-labels I(n), II, or *N,N,N*-trimethyl-*N*-tempoylammonium bromide were added to phospholipid suspensions (5% lipid, w/v) before or after sonication. For experiments designed to qualitatively demonstrate membrane permeation, the sonication medium contained 150 mM K^+, 300 mM Na^+, 225 mM SO_4^{2-} plus 50 mM sodium phosphate buffer, pH 6.8. The sonicated vesicles, containing label added either before or after sonication, were cooled to 0 °C and sodium ascorbate and $FeSO_4$ were added to final concentrations of 11 mM and 10 mM, respectively. The samples were immediately placed in a temperature controlled EPR cavity at 0 ± 0.1 °C and the signal was monitored as a function of time. For experiments designed to quantitate the internal–external distribution of label, spin label II (5×10^{-5} M) was added to sonicated vesicles (3%, w/v) under conditions of zero and high inside-negative potential prepared as described above for a $(K^+)_{in}/(K^+)_{out}$ of 90/1 without and with valinomycin, respectively. The samples were cooled to 0 °C, ascorbate and $FeSO_4$ added as above and the spectra recorded in the temperature-controlled cavity.

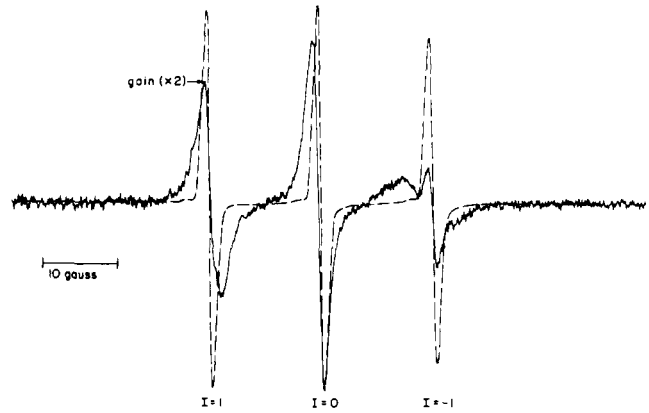

FIGURE 1: EPR spectra of samples containing 2×10^{-5} M spin label I(3) in aqueous solution (- - -) and in the presence of 15% (w/v) PC vesicles (—). In both cases, the samples contained 225 mM K^+, 225 mM Na^+, 225 mM SO_4^{2-}, and 50 mM sodium phosphate buffer, pH 6.8. The EPR spectrometer gain for the label in the presence of vesicles was set twice that for the label free in solution.

Results

Potential-Dependent Binding of Phosphonium Spin Labels to Phospholipid Vesicles. The mean diameter and standard deviation of the sonicated phospholipid vesicles used in these experiments were 300 Å and 40 Å, respectively, as determined by electron microscopy of negatively stained preparations. Figure 1 shows EPR spectra of spin label I(3) in aqueous solution and in the presence of phospholipid vesicles. In the latter case, the spectrum is clearly a superposition of a broad and narrow component. This spectrum closely resembles that reported by Castle and Hubbell (1976) for the equilibrium binding of the cationic spin label *N,N*-dimethyl-*N*-nonyl-*N*-tempoylammonium bromide to phospholipid vesicles in aqueous solution. The broad spectral component in Figure 1 arises from label I(3) bound to vesicles while the narrow component arises from the label free in aqueous solution. The two populations ("bound" and "free") of spin label are apparently in equilibrium; that is, they are inversely related to each other when vesicle concentration is varied. At sufficiently high vesicle concentrations, the narrow component is essentially absent and a pure bound spectrum remains. Using this sample of totally bound I(3) together with a sample of I(3) in the absence of vesicles, composite spectra essentially identical in shape with those given in Figure 1 can be produced by recording the spectrum of both samples simultaneously as described by Castle and Hubbell (1976). This result strongly supports the contention stated above that the spectra of I(3) in the phospholipid vesicle suspension are a simple summation of a free and bound component. The ratio of bound-to-free spin populations at equilibrium is readily obtained from the spectra as outlined in the experimental section.

Valinomycin is known to produce transmembrane potentials when a gradient of K^+ exists across the wall of phospholipid vesicles (Eisenman et al., 1975). Figure 2 shows the EPR spectra of I(3) in a phospholipid vesicle suspension with 450 mM K^+ in the vesicle internal volume and 450 mM Na^+ in the external solution in the presence and absence of valinomycin.

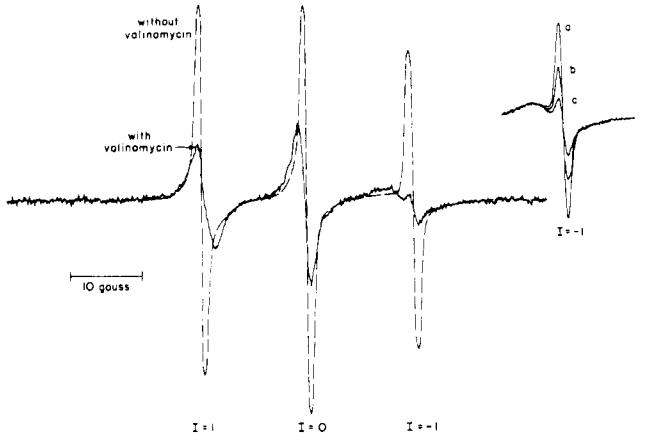

FIGURE 2: EPR spectra of 2×10^{-5} M I(3) in a 2% (w/v) vesicle preparation with (—) and without (- - -) 1 μM valinomycin. The interior vesicle volume contained 450 mM K^+, 225 mM SO_4^{2-} plus 50 mM sodium phosphate buffer, pH 6.8, while the external solution contained 450 mM Na^+, 225 mM SO_4^{2-} plus 50 mM sodium phosphate buffer, pH 6.8. Inset: The high field resonance, $I = -1$, from spin label I(3) in the presence of PC vesicles (2% w/v) and 1 μM valinomycin at three ratios of K_{in}^+/K_{out}^+: (a) 3/1; (b) 10/1; (c) 45/1. The intensity decrease in the sharp component of $I = -1$ represents a decrease of spin label in the aqueous phase. The concomitant increase in bound signal is not detectable due to the large width of this resonance line.

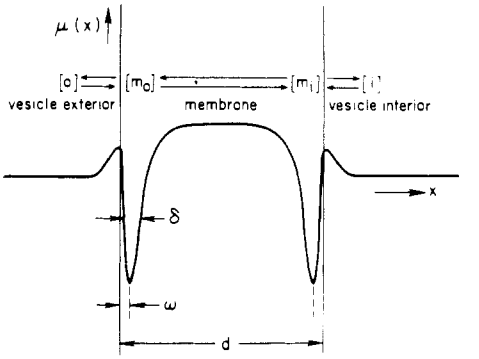

FIGURE 3: Potential energy profile across a bilayer membrane for a hydrophobic ion in the absence of a transmembrane electric potential (Ketterer et al., 1971). ω is the internal displacement of the potential minima from the membrane surface, δ is the effective width of the potential wells, d is the membrane thickness, and $\mu(x)$ is the potential energy of the ion. o, m_o, m_i, and i represent four discrete regions occupied by the ion: the exterior solution; the exterior interface; the interior interface; and the vesicle interior volume, respectively.

The dramatic increase in the fraction of bound I(3) in the presence of the ionophore suggests that the binding equilibria are potential dependent. When I(3) is added to vesicles with a potential already established across the membrane, equilibrium is reached in a time short compared to the resolution of the procedure, i.e., approximately 30 s. Valinomycin in the absence of a K^+ gradient ($(K^+)_{in}/(K^+)_{out} = 1$) produces no detectable spectral changes. Furthermore, as will be discussed in detail below, the equilibrium populations of bound and free spins are continuous, predictable functions of the K^+ gradient in the presence of the ionophore. The spectral changes produced by valinomycin are relatively stable in time, the bound fraction decreasing by only about 10% over 8 h at room temperature. However, the addition of 10 μM gramicidin S causes an immediate return of the spectrum to the zero potential state. The above results indicate that perturbations of the binding equilibria of I(3) by valinomycin are not due to effects of the antibiotic alone, but rather are the result of a transmembrane potential established by a selective K^+ permeability increase.

Permeability of Phospholipid Vesicles to Phosphonium Nitroxides. At 0 °C sonicated liposomes are impermeable to sodium ascorbate, a powerful reducing agent for nitroxide radicals (Kornberg and McConnell, 1971). When phosphonium labels I(n) and II are added to *previously sonicated vesicles* and allowed to equilibrate ca. 5 min at room temperature, the vesicle suspension is cooled to 0 °C, and ascorbate added, it is found that the majority of the spin is rapidly reduced leaving behind a small population of more slowly reducing spin. The initial amount of spin in this latter population is consistent with that expected from the total internal volume of the vesicles (see below) and decays according to first-order kinetics with a half-life of 50 min for I(3) and 8 min for II. When the same experiment is performed with the positively charged nitroxide *N,N,N*-trimethyl-*N*-tempoylammonium bromide, all the spin is reduced essentially instantaneously. When phosphonium labels I(n) and II are present *during sonication* in the vesicle preparation, the vesicles cooled to 0 °C, and ascorbate is added, results identical with those described above for phosphonium labels added *after* sonication are obtained. On the other hand, for vesicles to which *N,N,N*-trimethyl-*N*-tempoylammonium bromide was added during sonication, ascorbate reduction at 0 °C reveals the presence of a small population of very stable spin with a half-life greater than 6 h. This latter experiment is in accord with the fact that phospholipid vesicles trap small molecules present during sonication (Kornberg et al., 1972) and further confirms the impermeability of the vesicles to both ascorbate and the quaternary ammonium nitroxide. The observation of the same "protected" population for phosphonium nitroxides added before or after sonication qualitatively demonstrates the permeability of the phosphonium labels. The fact that the protected population is slowly reduced suggests a finite membrane permeability even at 0 °C.

Thermodynamic Analysis of Potential-Dependent Binding Equilibria. Large hydrophobic organic ions have been shown to bind to interfacial regions of phospholipid bilayers and rapidly penetrate the low dielectric membrane interior (Ketterer et al., 1971; Anderson and Fuchs, 1975). The spin labels I(n) and II are paramagnetic derivatives of the hydrophobic ion methyltriphenylphosphonium, and it is thus not surprising that these molecules show binding to phospholipid vesicles, high membrane permeability, and potential dependent phenomena. Following the lead of earlier work, we assume a potential energy function of the type shown in Figure 3 for the transit of the hydrophobic ion across the bilayer. The potential minima at the interfaces are characteristic for the interaction of hydrophobic ions with lipid bilayers and correspond to binding regions for the charged moieties of I(n) and II at m_i and m_o. A profile of this form is physically plausible and is consistent with data on the permeation kinetics of hydrophobic ions (Ketterer et al., 1971; Anderson and Fuchs, 1975). Thus in vesicle suspensions appreciable concentrations of the charged moieties of I(n) and II are expected to be found in the four regions of space identified as o, m_o, m_i, and i in Figure 3. In the following analysis these regions will be regarded as separate "phases", and "binding" of the hydrophobic ion to the membrane will be viewed as equilibration of the ion between aqueous and membrane phases. At equilibrium in the presence of a transmembrane potential, the electrochemical potential ($\tilde{\mu}$) of the label in each region j (j = o, m_i, m_o, i) can be written

$$\tilde{\mu}_j = \mu_j^\circ + RT \ln \gamma_j \chi_j + ZF\psi_j$$

where: μ_j° is the chemical potential in the region j in the

Henry's law standard state in the absence of electric potentials; χ_j is the mole fraction of the charged group in the region j; γ_j is the activity coefficient of the label in region j; ψ_j is the electric potential in region j, and Z, F, R, and T are the valence of the label, the Faraday constant, the universal gas constant, and the temperature, respectively. ψ_0 will be taken as the reference potential; i.e., $\psi_0 \equiv 0$. Thus $\psi_i = \Delta\psi$, the transmembrane potential difference. In all experiments to be presented here, the ionic strengths of the vesicle interior and exterior solutions are the same, although specific ion gradients exist. Under these conditions, we will make the approximation that all activity coefficient ratios γ_j/γ_k are unity. Furthermore, in dilute solutions of I(n) or II, we will make the approximation that

$$\chi_j/\chi_k = \frac{n_j}{n_k}\frac{V_k}{V_j}$$

where n_j, n_k are the mole numbers of label in regions j and k and V_j and V_k are the corresponding volumes of those regions per vesicle. The volumes V_{m_o} and V_{m_i}, the effective volumes of the membrane phases, are unambiguously defined as the volumes of those regions of space occupied by phosphonium groups giving rise to a bound signal. If the probe associates with the membrane interface so that its charged moiety is in a region which is also accessible to ions in the aqueous phase, then $\psi_{m_o} = \psi_o$ and $\psi_{m_i} = \psi_i$.[2] However, if the location of the binding region is removed from the surface toward the bilayer interior, the probe will not experience the same potential as ions in the bulk aqueous phase. If ω is taken as the displacement of the binding region from the plane of the ions responsible for the creation of the potential and d is the bilayer thickness, we define $\alpha \equiv \omega/d$ (see Figure 3). In the constant field approximation, $\psi_{m_o} = \alpha\Delta\psi$ and $\psi_{m_i} = (1-\alpha)\Delta\psi$. In this analysis, α will be assumed to be potential independent. With the above approximations, definitions and the equilibrium conditions that $\tilde{\mu}_j = \tilde{\mu}_k$ for all regions (j, k), the following general expression for the ratio (moles spin bound)/(moles spin free) may be readily derived:

$$\frac{n_{m_i} + n_{m_o}}{n_o + n_i} = \frac{N_b}{N_f} = \frac{V_{m_i}}{V_i} \times \left[\frac{K_{m_i}e^{\alpha ZF\Delta\psi/RT} + K_{m_o}\frac{V_{m_o}}{V_{m_i}}e^{ZF(1-\alpha)\Delta\psi/RT}}{1 + V_o/V_i e^{ZF\Delta\psi/RT}}\right] \quad (1)$$

where: n_{m_o}, n_{m_i}, n_o, and n_i are the moles of spin at equilibrium in the four regions of space defined in Figure 3, N_b and n_f are the total numbers of bound and free spin, respectively, and K_{m_o} and K_{m_i} are the partition coefficients for the labels to the external and internal vesicle surfaces in the absence of a transmembrane potential; i.e., $K_{m_o} = e^{-\Delta\mu_{m_o}^\circ/RT}$ and $K_{m_i} = e^{-\Delta\mu_{m_i}^\circ/RT}$, where $\Delta\mu_{m_i}^\circ$ and $\Delta\mu_{m_o}^\circ$ are the corresponding unitary free energies of transfer for the ion from the bulk aqueous phase to the membrane phase. For the particular case of the compositionally symmetrical membranes described here we will take $K_{m_o} = K_{m_i} = K$. The validity of this assumption will be discussed further below. Thus for the present purposes eq 1 may be simplified to

$$N_b/N_f = K\frac{V_{m_i}}{V_i} \times \left[\frac{e^{\alpha ZF\Delta\psi/RT} + V_{m_o}/V_{m_i}\, e^{ZF(1-\alpha)\Delta\psi/RT}}{1 + V_o/V_i e^{ZF\Delta\psi/RT}}\right] \quad (2)$$

Equations 1 and 2 have been written in terms of the ratio of (*total* bound spin)/(*total* free spin) since in general the paramagnetic resonance spectrum alone cannot distinguish between spins in regions o and i or between spins in regions m_o and m_i and thus reports only the total populations.

Estimation of Thermodynamic Parameters. To test eq 2 using experimental data for N_b/N_f in the presence of known transmembrane potentials, values are needed for V_o/V_i, KV_{m_i}/V_i, V_{m_o}/V_{m_i}, and α. Experimentally, we find $V_o/V_i = 37$ in 5% (w/v) vesicle suspensions by the sucrose entrapment method described in the Experimental Section. The ratio V_o/V_i may be written as

$$V_o/V_i = \frac{V_t}{m_l}\frac{1}{\bar{V}_i} - \left[\frac{\bar{V}_l}{\bar{V}_i} + 1\right] \quad (3)$$

where: V_t is the total volume of the vesicle suspension; m_l is the mass of lipid in the suspension; $\bar{V}_i$ and $\bar{V}_l$ are the volumes of internal space and hydrated lipid bilayer per g of lipid, respectively. A value of 0.9885 mL/g for $\bar{V}_l$ has been reported (Huang, 1969) for egg phosphatidylcholine. Using this value together with $V_o/V_i = 37$ for 5% vesicles ($V_t/m_l = 20$ mL/g), the intensive quantity $\bar{V}_i$ is estimated as 0.50 mL/g. With this value of $\bar{V}_i$, V_o/V_i for any vesicle suspension may be computed from the composition and eq 3.

Experimental values of KV_{m_i}/V_i may be outlined from a study of the binding of the labels to vesicles as a function of vesicle concentration in the absence of a potential. For the equilibrium binding of a molecule to discrete regions m_i and m_o of volume V_{m_i} and V_{m_o}

$$\frac{N_b}{N_f} = K\frac{V_{m_i}}{V_i}\left[\frac{1 + V_{m_o}/V_{m_i}}{1 + V_o/V_i}\right] \quad (4)$$

which is identical to eq 2 with $\Delta\psi = 0$. Substitution of V_o/V_i in eq 4 by eq 3 gives

$$\frac{N_f}{N_b} = \frac{V_t}{m_l}\frac{1}{\bar{V}_i\beta} - \frac{1}{\beta}\frac{\bar{V}_l}{\bar{V}_i} \quad (5)$$

where

$$\beta = K\frac{V_{m_i}}{V_i}[1 + V_{m_o}/V_{m_i}]$$

Thus a plot of experimental data for N_f/N_b vs. V_t/m_l for labels in equilibrium with vesicles should yield a straight line of slope $1/\bar{V}_i\beta$. Figure 4 shows data plotted in this fashion for labels I(2) and I(3) in equilibrium with vesicles with no transmembrane potential.[3] The plots are indeed linear with slopes of 0.023 and 0.057 g/mL for I(3) and I(2), respectively. To determine KV_{m_i}/V_i from the slope, V_{m_o}/V_{m_i} must be estimated. V_{m_o}/V_{m_i} (and hence KV_{m_i}/V_i) is a function of α, the only adjustable parameter which appears in the theory. The functional

[2] As written, these equalities appear to hold only in the absence of interfacial potentials due to sources such as surface and dipole potentials. However, it will be shown below that such potentials simply modify the apparent binding constant of the phosphonium ions to the membrane. To simplify the notation at this point, these potentials are not explicitly included in eq 1 and 2 below, but instead are incorporated in the zero-transmembrane potential partition coefficients K_{m_o} and K_{m_i}. The effects of interfacial potentials will be examined in detail in the Discussion.

[3] Caution must be exercised in these zero-potential measurements since the permeable spin label itself gives rise to transmembrane potentials. Our measurements were restricted to high vesicle concentrations and low spin-label concentrations to minimize this error. Under the conditions of Figure 4, the maximum error contributed by this source cannot exceed ca. 5%, and no corrections to the data were attempted.

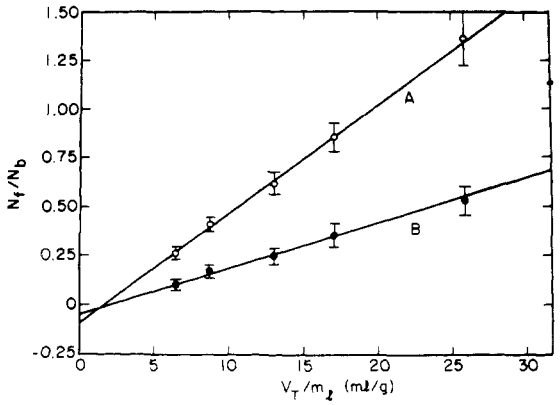

FIGURE 4: Equilibrium binding of I(2) (A, open circles) and I(3) (B, solid circles) to phospholipid vesicles in the absence of a transmembrane potential. The ratio of free:bound label (N_f/N_b) is plotted vs. the total volume per mass lipid (V_t/m_l). Vesicles of different concentration all contained 225 mM Na^+, 225 mM K^+, 225 mM SO_4^{2-} plus 50 mM sodium phosphate buffer, pH 6.8. The slopes for the binding curves of I(2) and I(3) are 0.057 and 0.023 g/mL, respectively.

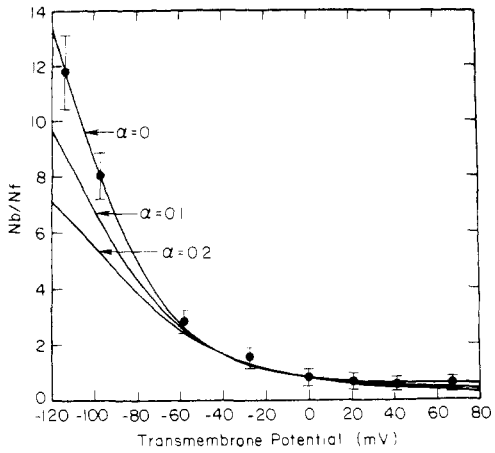

FIGURE 5: Calculated and experimentally determined values of N_b/N_f as a function of transmembrane potential, $\Delta\psi$. The three solid lines represent the theoretical dependence of N_b/N_f upon $\Delta\psi$ calculated from eq 2 for three values of α. The parameters V_{m_o}/V_{m_i} and KV_{m_i}/V_i used in the calculation were computed for each value of α as described in the text; V_o/V_i was 108, corresponding to 1.8% (w/v) PC vesicles. The solid circles (●) represent ratios of N_b/N_f determined experimentally in 1.8% (w/v) PC vesicles for several values of $\Delta\psi$.

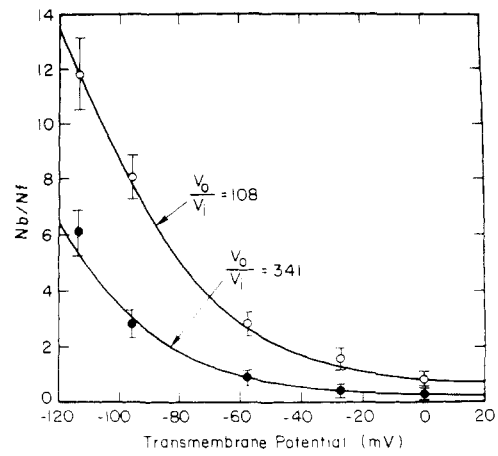

FIGURE 6: A plot showing the calculated and experimentally determined values of the ratio bound:free (N_b/N_f) for I(3) in vesicle suspensions as a function of transmembrane potential for V_o/V_i = 108 and V_o/V_i = 341. The solid lines (—) are the values of N_b/N_f computed from eq 2 for the two values of V_o/V_i with α = 0, V_{m_o}/V_{m_i} = 2.3, and KV_{m_i}/V_i = 26.2. The latter value was obtained from the slope of the binding curve for I(3) (Figure 4) and eq 5. Experimental data for V_o/V_i = 108 and V_o/V_i = 341 are shown as open (○) and solid (●) circles, respectively.

relationship between these quantities depends on vesicle geometry and the width of the potential wells in the membrane. A simple relationship can be derived for spherical vesicles by considering V_{m_o} and V_{m_i} to be spherical shells centered at ω and of effective thickness δ (see Figure 3). In this case

$$\frac{V_{m_o}}{V_{m_i}} = \left[\frac{(r_o - \alpha d + \delta/2)^3 - (r_o - \alpha d - \delta/2)^3}{(r_o + d(\alpha - 1) + \delta/2)^3 - (r_o + d(\alpha - 1) - \delta/2)^3}\right] \quad (6)$$

where r_o is the outer radius of the vesicle. The mean vesicle diameter estimated from electron microscopy is 300 Å and r_o = 150 Å. The full bilayer thickness (choline-to-choline) for egg PC is ca. 50–52 Å as estimated from electron density profiles (Levine and Wilkins, 1971) and molecular models. The potential minima are assumed to be well defined, and δ may be taken to be approximately equal to the dimensions of the charged portions of the hydrophobic cation, i.e., about 4 Å. The results are not very sensitive to the choice of δ and any value between 2 and 8 Å could equally well be used. With these estimates, V_{m_o}/V_{m_i} may be obtained from eq 6 and then KV_{m_i}/V_i obtained from the slopes of the binding curves (eq 5) and eq 2 tested with α as the only adjustable parameter.

Figure 5 shows experimental values of N_b/N_f for I(3) in equilibrium with vesicles at various transmembrane potentials. Also shown are plots of eq 2 at three different values of α, and, to within experimental error, the data are well accounted for by eq 2 with α = 0. Actually, the precision of the data only allows the conclusion $0 \leq \alpha \leq 0.04$, but for simplicity in the calculations to follow, α will be taken as zero. In any case, these small values of α correspond to binding regions very close to the polar surface of the bilayer. Equation 2 predicts that the potential dependence of N_b/N_f should be a function of V_o/V_i, a variable easily manipulated simply by changing the vesicle concentration (eq 3). Figure 6 shows both the experimental data for N_b/N_f as a function of $\Delta\psi$ for two values of V_o/V_i and the dependence predicted using eq 2. The close agreement of calculated and experimental values further supports the validity of the simple model expressed by eq 2.

The general equations 1 and 2 are written in a form to give the observable quantity N_b/N_f extracted directly from the EPR spectra. However, an important prediction of the equilibrium model is that the spin populations n_{m_i} and n_{m_o} are simply related by

$$\frac{n_{m_i}}{n_{m_o}} = \frac{V_{m_i}}{V_{m_o}} e^{-\Delta\psi ZF/RT} \quad (7)$$

This prediction cannot be verified by observation of spectra from equilibrium states since only the total free and total bound populations are distinguishable. To estimate the individual populations n_{m_i} and n_{m_o}, we have taken advantage of the properties of label II. This hydrophobic ion has a membrane partition coefficient such that the free label concentration at equilibrium is very small, near the limit of detection of the spectrometer. Thus, the spectra obtained for II in vesicle suspensions reflect only the total bound population $n_{m_o} + n_{m_i}$. Resolution of the total signal into components arising from spins bound to regions m_o and m_i can be achieved by selective reduction of the externally located population with ascorbate at 0 °C. Even at this temperature, however, the internally

trapped phosphonium label is able to penetrate the bilayer as shown above. Hence, addition of ascorbate to vesicles at 0 °C in equilibrium with II should reveal two reduction rates, one rapid rate corresponding to the reduction of external label and another slower rate corresponding to the migration of II across the membrane with subsequent fast reduction. Figure 7 shows the reduction kinetics of label II in vesicle suspensions at 0 °C in the presence of external ascorbate for vesicles with a 0 and −113 mV potential difference across the membrane. As anticipated, two kinetic populations are observed in each case. The initial reduction is too rapid to be accurately followed by the procedures used, and only the important slow reduction is analyzed in Figure 7.[4] The slow reduction reactions in each case appear to obey first-order kinetics over the time range studied, and extrapolation to zero time yields values of 0.98 and 0.32 for the fractions of total label in the slowly reducing population for $\Delta\psi = -113$ and 0 mV, respectively. The simple Nernst distribution predicts that n_{m_i} should amount to 0.98 and 0.30 of the total bound spin at −113 and 0 mV, respectively, in excellent agreement with the experimentally estimated populations of slowly reducing label. Figure 7 shows that the reduction rate constant in the vesicles with $\Delta\psi = -113$ mV is approximately a factor of 7 slower than in vesicles with $\Delta\psi = 0$ mV. This is expected since the outward migration of the label in the former case is against the electric field gradient.

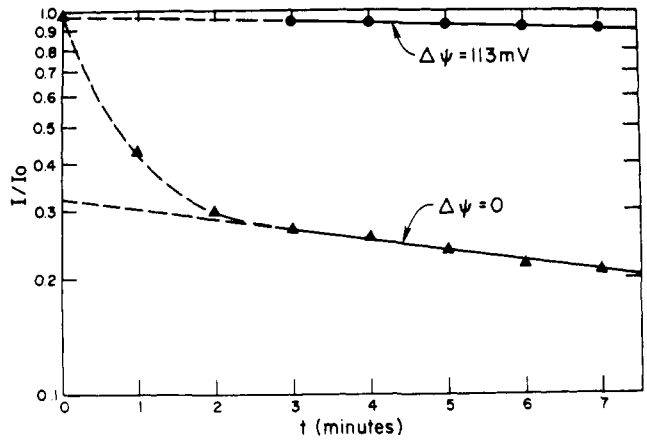

FIGURE 7: Reduction of 5×10^{-5} M spin label II after ascorbate addition under the following conditions: (▲) 3% (w/v) PC vesicles, $\Delta\psi = 0$; (●) 3% (w/v) PC vesicles, $\Delta\psi = -113$ mV. Spin label II was added to sonicated vesicles and allowed to equilibrate for approximately 5 min at room temperature. Ascorbate was then added at 0 °C and the fraction of the remaining low field resonance intensity (I/I_0) was followed as a function of time.

Discussion

Considering the approximations made, the simple theory proposed here accounts rather well for the binding equilibria of I(n) as a function of transmembrane potential and vesicle concentration and allows the determination of absolute transmembrane potentials if certain intensive properties of the vesicles are determined independently. An assumption of this theory is that the potential profile for the labels in the absence of a transmembrane electric potential is qualitatively similar to that shown in Figure 3. Implicit in this assumption is the condition that the central barrier be sufficiently high to ensure that the number of spins in the membrane interior be much lower than the number in o, m_o, m_i, or i. We do not, however, make any assumptions regarding the detailed shapes of the potential barriers. A profile of this form is expected on theoretical grounds (Ketterer et al., 1971) and has strong experimental support (Ketterer et al., 1971; Anderson and Fuchs, 1975). Data obtained in the present experiments are also consistent with this model. For example, the ratios of the slopes of the binding curves for I(2) and I(3) given in Figure 4 are just equal to the ratios of the partition coefficients for the two molecules, i.e.

$$\left(\frac{1}{\bar{V}_i\beta}\right)_{n=3} \Big/ \left(\frac{1}{\bar{V}_i\beta}\right)_{n=2} = \frac{K_{n=2}}{K_{n=3}} = e^{-[\Delta\mu^\circ(2)-\Delta\mu^\circ(3)]/RT}$$

Thus, the difference in the free energy of transfer of I(2) and I(3) from water to the membrane binding region is found to be ca. 500 cal/mol. Since these labels differ by only one methylene group, this represents the unitary free energy of transfer per mole of methylene group from water to the membrane binding region. Tanford (1973) has shown that the free energy of transfer per mole of methylene group from water to liquid hydrocarbon is generally on the order of 700 cal/mol. Assuming that the incremental free energies are largely structure independent, this implies that the membrane binding region for the hydrophobic ions is more polar than the membrane interior, consistent with the interfacial location of the potential minima as shown in Figure 3. furthermore, the experimental data are fit by eq 2 with α close to zero, consistent with an interfacial binding region.

It has been assumed that the potential profile for the transit of I(n) across the membrane is symmetric with respect to the center of the bilayer in the absence of electric potentials. Since phospholipid packing densities on the outer and inner surfaces of the bilayer in small vesicles are different (Chan et al., 1973), the potential profile cannot in reality be perfectly symmetric. However, the EPR spectral lineshapes of the *bound* label are very similar at zero and high negative applied potentials. Since the populations of spin in the inner and outer membrane phases are very dependent on potential, this result implies that the environment of the label is similar in the inner and outer phases, and we approximate the membrane as a symmetrical structure with respect to the membrane partition coefficient for I(n). Furthermore, if the partition coefficients for the two surfaces were different, one would expect $K_{m_i} < K_{m_o}$ due to the higher packing density on the interior surface. However, this would lead to significantly *lower predicted* values of N_b/N_f at high potentials and would require *smaller* values of α to achieve a tolerable fit with the data. Since α is already essentially zero for the best fit, this seems improbable. The ultimate justification for the assumed uniform partition coefficient lies in the reasonable agreement of the experimental data with theoretical expectations based on this assumption.

Equations 1 and 2 are written in terms of unitary free energies and are applicable in the dilute solution region where ratios of mole fractions are approximately equal to ratios of molar concentrations of I(n). The highest concentration of label will be found in the vesicle internal membrane surface at high potentials in dilute vesicle suspensions. Such a situation is found, for example, at $\Delta\psi = -120$ mV in suspensions where $V_o/V_i = 340$ (see Figure 5). At this vesicle concentration and a total spin concentration of 2×10^{-5} M, there are approximately 15 total spins per vesicle. At $\Delta\psi = -120$ mV, $N_b/N_f = 6.3$ for I(3) and $N_b = 13$. If essentially all 13 bound spins

[4] Even though the nitroxide group of II is buried deep within the bilayer when membrane-bound, reduction of the external label occurs since the probe is in equilibrium with a small but finite population in the aqueous phase. The rapid initial reduction of spin upon ascorbate addition suggests that the "off" rate from the membrane to the aqueous solution is fast compared with the transmembrane migration rate at 0 °C. The rate constant for reduction of aqueous spin is in turn fast compared to the "off" rate.

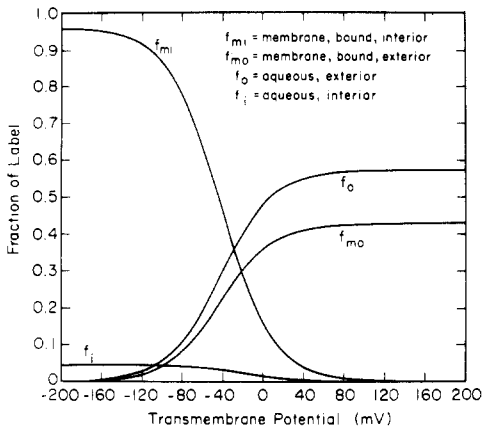

FIGURE 8: Theoretical distribution of a hydrophobic cation in the regions o, m_o, m_i, and i (see Figure 3) as a function of transmembrane potential. f_o, f_{m_o}, f_{m_i}, and f_i are the fractions of *total* label residing in each of the respective regions. This distribution has been calculated for V_{m_o}/V_{m_i} = 2.3, V_o/V_i = 70, α = 0, and KV_{m_i}/V_i = 20.

were at the internal surface, the effective concentration of I(3) in a 4-Å shell would be 0.04 M. This is the worst situation, but even at this concentration the dilute solution approximation is tolerable since the concentration of lipids in this phase is at least two orders of magnitude greater. Generally the experiments are conveniently carried out with vesicle suspensions with $V_o/V_i \simeq 100$ (2% w/v lipid) where there are ca. 4 spins per vesicle and local concentrations in the membrane never exceed 0.01 M in realistic ranges of potential. At a 2×10^{-5} M total spin concentration and $V_o.V_i = 100$, the concentration of spin in the interior vesicle aqueous volume approaches a maximum of $\sim 10^{-4}$ M as the potential approaches infinity, inside negative.

To express eq 2 with the minimum number of independent parameters, the geometry of the vesicle must be known and we have assumed a spherical shape. Sonicated vesicles of the type used here have been well characterized, and electron microscopy and hydrodynamic properties (Huang, 1969) are consistent with a spherical shape. Furthermore, the calculated internal volume per gram of lipid ($\bar{V}_i$) for spherical vesicles is 0.5 mL/g,[5] the same as that found experimentally, and the assumption of spherical vesicles seems justified.

At this point it is appropriate to briefly comment on the approaches used to arrive at experimental values for $\Delta\psi$ and N_b/N_f. The expected values of $\Delta\psi$, corresponding to known K^+ concentration gradients, were calculated assuming an ion selectivity of valinomycin sufficiently high so that $P_{Na^+}/P_{K^+}(Na^+) \ll (K^+)$ for both the internal and external solutions. This assumption is commonly made and seems reasonable since, in PC bilayers, valinomycin is expected to operate in the "equilibrium domain" where $P_{Na^+}/P_{K^+} \sim 10^{-4}$ to 10^{-5} (Eisenman et al., 1975; Eisenman, personal communication). The fact that the transmembrane potentials generated with valinomycin change very little over a period of 8 h at room temperature suggests the very high cation selectivity of the ionophore as well as the impermeability of the SO_4^{2-} anion used in our experiments. Since the addition of CCCP to vesicles at high transmembrane potentials produces no change in the EPR spectra of I(n) in vesicles, we assume that the membrane is permeable to protons, a conclusion reached earlier by Kornberg et al. (1972). If protons are in equilibrium across the membrane, the equilibrium value of $\Delta\psi$ will be less than predicted by the Nernst equation for the initial K^+ gradient by an amount dependent on the buffer concentration. For this reason, the actual values of potentials shown for experimental values of N_b/N_f in Figures 5 and 6 have been corrected for proton movement as described by Kornberg et al. (1972).

The approach taken here to estimate N_b/N_f from the EPR spectra has the important feature that it does not rely on any assumptions regarding the EPR line shape of the membrane bound signal. Thus, possible spin exchange interactions in the membrane phases or potential dependence of the bound line shape in no way affects the analysis. This procedure, however, requires the conservation of spin. In our experiments, no spin reduction was noted during the time required to complete any of the measurements. Other methods of spectral analysis, which may prove useful in systems where slow reduction is present, have been discussed by Castle and Hubbell (1976). Slight hydrolysis of the ester linkage of I(n) and II can lead to serious underestimates of N_b/N_f at high transmembrane potentials. To avoid this problem, it is imperative to use freshly prepared solutions of these nitroxides.

Equation 2 expresses the combined result of three coupled equilibria between n_o and n_{m_o}, n_{m_o} and n_{m_i} and n_{m_i} and n_i. The excellent agreement of the experimental data with eq 2 is strongly supportive but insufficient in itself to prove the equilibrium model upon which eq 2 is based. However, independent demonstration of the existence of the three equilibria more firmly establishes the model. The data of Figure 4, for example, quantitatively demonstrate the equilibrium binding of the probes to the membrane in the absence of electric potentials. The data of Figure 7 together with the known permeability of the probe directly demonstrate the $n_{m_o} = n_{m_i}$ equilibrium. Furthermore, the population ratios are in quantitative agreement with predictions. Taken together, these results leave little doubt as to the essential correctness of the model.

Physically, the method used to detect transmembrane potentials is based on the larger membrane surface-to-volume ratio of the interior vesicle space compared with that of the external solution. When the vesicle interior has a negative electric potential relative to the exterior, the positive hydrophobic ions migrate to this region and since there is more membrane phase per unit volume on the interior, the net amount of bound label increases. Figure 8 shows this behavior graphically in terms of the fractional populations of each of the regions of space occupied by labels as a function of transmembrane potential. Evidently, the sensitivity of the method will depend on the vesicle size, geometry, and concentration. The sensitivity, S, is defined as $S \equiv \partial(N_b/N_f)/\partial\Delta\psi$, and

$$S = K\frac{V_{m_i}}{V_i}\frac{ZF}{RT}e^{+\Delta\psi ZF/RT}\left[\frac{V_{m_o}/V_{m_i} - V_o/V_i}{(1 + V_o/V_i e^{\Delta\psi ZF/RT})^2}\right]$$

Notice when $V_{m_o}/V_{m_i} = V_o/V_i$, $S = 0$. For an arbitrary vesicle size and geometry, the sensitivity increases linearly with the binding constant of the hydrophobic ion, a parameter which is readily controlled by varying the alkyl chain length of molecules of structure II. There are practical limitations; for example, if the binding constant is too large, the free signal becomes too small to detect. The variation of S with V_o/V_i shows a maximum at the point where

$$\frac{\partial}{\partial(V_o/V_i)}\left(\frac{\partial N_b/N_f}{\partial(\Delta\psi)}\right) = 0$$

[5] The mean outer diameter of the vesicles is 300 Å. Taking this as the diameter of a spherical structure and a bilayer thickness of 55 Å, the total membrane surface area per vesicle is 3.96×10^5 Å^2. The area occupied by a single lipid is ca. 70 Å^2 (Castle and Hubbell, 1976), giving about 5700 lipids per vesicle or 7.24×10^{-18} g of lipid using 770 as an average molecular weight for egg PC. The internal volume is calculated to be 3.59×10^{-18} mL, giving $\bar{V}_i$ = 0.5 mL/g.

Solution of this equation gives

$$(V_o/V_i)_{max} \approx e^{-\Delta\psi ZF/RT} + 2V_{m_o}/V_{m_i}$$

where $(V_o/V_i)_{max}$ is the value for maximum sensitivity. Thus, the vesicle concentration must be higher for maximum sensitivity at less negative potential ranges. For spherical vesicles of diameter 300 Å, eq 6 gives $V_{m_o}/V_{m_i} = 2.34$. For the data in Figure 5, $V_o/V_i = 108$, and the maximum sensitivity is predicted to occur at ca. −120 mV, a conclusion readily appreciated by examination of the data.

In general, the hydrophobic ions I(n) and II will also be influenced by interfacial potentials at m_o and m_i such as those due to dipole effects or surface charges, and in certain situations this effect can dramatically alter the transmembrane potential dependence of the EPR spectra. The presence of constant interfacial potentials, ϕ, will simply alter the zero-transmembrane-potential binding constants by a factor of $e^{-\phi ZF/RT}$, and eq 1 (with $\alpha = 0$) may be written to include this effect as follows:[6]

$$\frac{N_b}{N_f} = \frac{V_{m_i}}{V_i} \times \left\{ \frac{K_{m_i}' e^{-ZF\phi_i/RT} + V_{m_o}/V_{m_i} K_{m_o}' (e^{-ZF\phi_o/RT})(e^{\Delta\psi ZF/RT})}{1 + V_o/V_i e^{ZF\Delta\psi/RT}} \right\}$$

where ϕ_i and ϕ_o are the total interfacial potentials of the inner and outer membrane surfaces due to sources independent of transmembrane potential, respectively, and K_{m_i}' and K_{m_o}' are the true zero-potential partition coefficients to the membrane surfaces. Notice that $K_{m_i} = K_{m_i}' e^{-\phi_i ZF/RT}$ and $K_{m_o}' \cdot e^{-\phi_o ZF/RT}$ where K_{m_i} and K_{m_o} are those appearing in eq 1. If $\phi_i < \phi_o$, the sensitivity per unit binding constant increases, while if $\phi_i > \phi_o$ the sensitivity per unit binding constant decreases. In fact, N_b/N_f becomes potential *independent* when

$$(\phi_i - \phi_o) = \frac{RT}{ZF} \ln \left[\frac{V_o}{V_i} \frac{V_{m_i}}{V_{m_o}} \frac{K_{m_i}}{K_{m_o}} \right]$$

Physically, this is due to the fact that the effect of the increased surface/volume on the interior of the vesicles is just offset by the decrease in binding due to the higher interfacial potential on the interior. For the vesicles used here, the interior interfacial potential would have to be more positive than the exterior by about 100 mV for N_b/N_f to become potential independent. For larger vesicles typical of isolated biological membrane fractions, smaller differences would suffice.

The basic mechanism of the potential sensitivity of spin labels I(n) and II in vesicles was in fact suggested some time ago by Bakeeva et al. (1970) to account for the changes in Ans fluorescence with energization of mitochondria. It also seems probable that the slow potential-dependent changes in fluorescence from cyanine and oxanol dyes in cells and vesicles originate from similar effects (Sims et al., 1974). However, it should be emphasized that, even if the potential-dependent redistributions of these dyes and the spin labels are similar, the mechanisms of *sensing* these redistributions are quite different. The fluorescence changes likely result from a concentration dependent aggregation (Sims et al., 1974), while the spin-label spectral changes arise from a simple population redistribution. Thus, while the fluorescence changes rely on the presence of a relatively large number of dye molecules in the volume of aggregation (Sims et al., 1974), the sensitivity of the spin label approach is independent of the total concentration of label and may be used with less than one molecule per vesicle.

In summary, we have developed a method for the estimation of transmembrane potentials in vesicles based on the potential-dependent equilibrium binding of hydrophobic spin-label ions. A simple thermodynamic theory is in quantitative agreement with experimental data obtained with sonicated phospholipid vesicles. These experiments lay the necessary foundation for future application to more interesting systems.

[6] For charged interfaces, this expression is accurate only for small surface potentials or conditions where the volumes of ionic double layers are small compared to the volumes of bulk aqueous phases.

Acknowledgments

The authors wish to thank Drs. George Eisenman, Alan Finkelstein, and David Castle for helpful discussions during the course of this work, Drs. Carole Hamilton and James Cason for the generous gifts of organic compounds, and Dr. Donald Glaser for allowing us unlimited use of his computer facilities.

References

Akerman, K. E., and Saris, N.-E. L. (1976), *Biochim. Biophys. Acta 426*, 624–629.

Akerman, K. E., and Wikström, M. (1976), *FEBS Lett. 68*, 191–197.

Anderson, O., and Fuchs, M. (1975), *Biophys. J. 15*, 795–829.

Bakeeva, L. E., Grinius, L. L., Jasaitis, A. A., Kuliene, V. V., Levitsky, D. O., Liberman, E. A., Severina, I. I., and Skulachev, V. P. (1970), *Biochim. Biophys. Acta 216*, 13–21.

Castle, J. D., and Hubbell, W. L. (1976), *Biochemistry 15*, 4818–4831.

Chan, S. I., Sheetz, M. P., Seiter, C. H., Feigenson, F. N., Hsu, M. C., Lau, A., and Yau, A. (1973), *Ann. N.Y. Acad. Sci. 222*, 499–522.

Chen, P. S., Toribara, T. Y., and Warner, H. (1956), *Anal. Chem. 28*, 1756–1758.

Denney, D. B., and Smith, L. C. (1962), *J. Org. Chem. 27*, 3404–3408.

Eisenman, G., Krasne, S., and Ciani, S. (1975), *Ann. N.Y. Acad. Sci. 264*, 34–60.

Folch, J., Lees, M., and Stone-Stanley, G. H. (1957), *J. Biol. Chem. 226*, 497–509.

Gaffney, B. J. (1976), in Spin Labeling Theory and Applications, Berliner, L. J., Ed., Academic Press, New York, N.Y., p 208.

Huang, C. (1969), *Biochemistry 8*, 344–351.

Keana, J. F. W., Keana, S. B., and Beetham, D. (1967), *J. Am. Chem. Soc. 89*, 3055–3056.

Ketterer, B., Neumcke, B., and Läuger, P. (1971), *J. Membr. Biol. 5*, 225–245.

Kornberg, R. D., and McConnell, H. M. (1971), *Biochemistry 10*, 1111–1120.

Kornberg, R. D., McNamee, M. G., and McConnell, H. M. (1972), *Proc. Natl. Acad. Sci. U.S.A. 69*, 1508–1513.

Levine, Y. K., and Wilkins, M. H. F. (1971), *Nature (London), New Biol. 230*, 69–72.

Sims, P. J., Waggoner, A. S., Wang, C.-H., and Hoffman, J. F. (1974), *Biochemistry 13*, 3315–3330.

Singleton, W. S., Gray, M. S., Brown, M. L., and White, J. L. (1965), *J. Am. Oil Chem. Soc. 42*, 53–56.

Stahl, E. (1969), Thin Layer Chromatography, 2nd ed, New York, N.Y., Springer-Verlag, p 904.

Tanford, C. (1973), The Hydrophobic Effect, New York, N.Y., Wiley.

Waggoner, A. S. (1976), *J. Membr. Biol. 27*, 317–334.